

Topology optimization design of microstructures with zero Poisson's ratio

Xueping Li, Jiajun Zhu, Peng Wei* , and Cheng Su

State Key Laboratory of Subtropical Building and Urban Science, School of Civil Engineering and Transportation, South China University of Technology, Guangzhou 510640, People Republic of China

Received: 1 March 2024 / Accepted: 14 May 2024

Abstract. Mechanical metamaterials are materials that possess unconventional mechanical properties that are not found in homogeneous materials, achieved through specific artificial microstructures. Topology optimization is an effective design method for such materials. In this paper, a topology optimization-based method for designing zero Poisson's ratio mechanical metamaterials is proposed. Firstly, a zero Poisson's ratio topology optimization objective function is constructed based on the energy homogenization method, and the optimal microstructure topology configuration and elastic coefficient matrix under different initial topologies and volume fractions are obtained through the boundary density evolution topology optimization method. To improve the saw tooth effect of the boundaries, the node density level set method is used to smooth the boundaries of the microstructure. Then, in finite element simulation analysis, it is demonstrated that the proposed method can effectively design microstructures with zero Poisson's ratio properties. It is also shown that microstructures with expected stiffness and zero Poisson's ratio properties can be obtained by changing the volume fraction and selecting materials with different stiffnesses. Finally, the unit cell is periodically arranged to form a multi-lattice metamaterial, and its zero Poisson's ratio mechanical performance in both X and Y directions is verified.

Keywords: Boundary density evolution / topology optimization / zero Poisson's ratio / microstructure / metamaterial

1 Introduction

As industrial products become more diverse, complex, and high-performance, traditional structural design can no longer meet the various needs of industrial products. Topology optimization, a novel design method, has become a common approach in the field. The theory of topology optimization design of microstructure unit cells in composite materials was first proposed by Sigmund in the mid-1990s [1]. It is an effective tool for seeking the optimal material distribution in the given design space. With breakthroughs in computer technology and the continuous improvement of mechanics theory, various topology optimization methods have gradually developed and become one of the leading design methods for super-material structures. Based on the idea that "structure determines performance" in materials science, super-materials, a particular type of material, can obtain properties that surpass those already existing in nature

through macro or micro-scale structural design [2,3]. As a new branch of research in the field of super-materials, mechanical super-materials try to obtain unconventional mechanical properties by employing specific artificial microstructures, such as negative Poisson's ratio [4,5] and zero Poisson's ratio materials [6]. Traditional materials usually exhibit positive Poisson's ratio effects, as shown in Figure 1a, where the material contracts transversely by a certain proportion under tension. However, for zero Poisson's ratio materials, as illustrated in Figure 1b, do not shrink or expand in another direction when stretched, making them widely researched due to their unique properties. Aerospace and defense industries, for instance, require the development of new materials with specific properties.

In Figure 1, L and L' denote the length of the material before and after deformation, B and B' denote the width of the material before and after deformation, and N denotes the axial tensile force on the material.

Olympic et al. [7] first designed a zero Poisson's ratio hexagonal honeycomb structure in 2010, derived the expressions of Young's modulus and shear modulus

* e-mail: ctpwei@scut.edu.cn

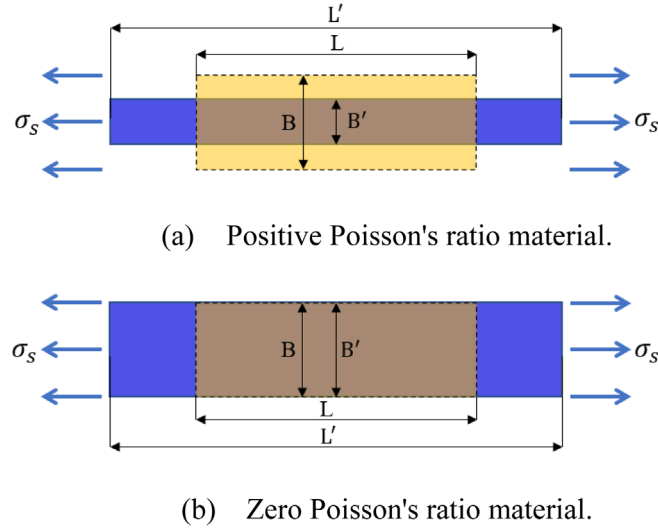


Fig. 1. The tensile deformation state of materials with positive and zero Poisson's ratio.

equivalent to the structure through theoretical analysis, and analyzed the effect of honeycomb parameters on its one-dimensional mechanical properties. Grima et al. [8] improved the existing hexagonal honeycomb structure in 2010 by proposing a semi concave honeycomb structure, and verified its zero Poisson's ratio characteristics through finite element analysis. Lu [9] and Li et al. [10] analyzed the equivalent elastic modulus and shear modulus of the honeycomb material proposed by Olympic et al. [7], derived the theoretical calculation formula for the equivalent elastic modulus in the plane of the zero Poisson's ratio honeycomb core, and compared the calculation results with the finite element experimental results to verify the correctness of the formula. Simone et al. [11] designed a hybrid zero Poisson's ratio honeycomb structure in 2017 by alternating orthogonal hexagonal and concave hexagonal honeycomb structures. Through compression tests, it was found that the compressive strength of the structure is twice that of the original structure, under the condition of constant in-plane stiffness. Gong et al. [12] proposed a quadrangular star-shaped zero Poisson's ratio honeycomb structure that can realize deformation in two orthogonal directions. Cheng et al. [13] classified cells based on the type of straight arms and proposed a cross shaped mixed zero Poisson's ratio honeycomb cell, and analyzed the mechanical properties of the structure. Chang et al. [14] designed inverse from the nature of the material, first selected the value of Poisson's ratio of the microstructure, and then through the continuous optimization of the microstructure finally obtained the microstructure with the target Poisson's ratio. Hamzehei et al. [15] introduced a new 4D zero Poisson's ratio metamaterials fabricated through the 3D printing technology, and through the experiments of the new material and the traditional 3D folded metamaterials were compared concerning the energy absorption ability, which proved the mechanical properties

of the new material. Chen et al. [16] built in-plane negative Poisson's ratio and out-of-plane zero Poisson's ratio 3D structures based on 2D parallelogram honeycomb by structural splicing and verified them by using finite element simulations and experiments. Gaal et al. [17] constructed a new zero Poisson's ratio structure by using two parallel rigid rods and flexible springs connecting the rigid rods. They discussed the possibility of extending the model to three-dimensional structures with compression in any direction, and also discussed the advantages and disadvantages of these models.

From the analysis of the existing research results, it can be seen that there are many mature research works on zero Poisson's ratio structural design, but most of them are based on honeycomb structure, and there are fewer studies combining both topology optimization and zero Poisson's ratio microstructural design.

Clausen et al. [18] proposed a simplified design consisting of a set of parameter hyperellipsoids, where the length of each hyperellipsoid is controlled by the design point. Then, shape optimization was used to fine tune the hyperellipsoid design. A series of honeycomb structures with Poisson's ratios ranging from -0.8 to 0.8 were optimized, and experimental verification was conducted to verify that the structure maintains a constant Poisson's ratio even under large deformations; However, the drawback of this method is that it requires optimization of specific initial shapes, which has significant limitations. And topology optimization does not require any restrictions on the initial shape of the material, so it has a wider range of applications and is more in line with practical engineering needs. For example, Yang et al. [19] used a multi evaluation point functional primitive topology optimization method to design a zero Poisson's ratio structure. They defined two sub structures, positive and negative Poisson's ratios, in the same topology structure to

achieve the design of a zero Poisson's ratio structure. Then, they verified the zero Poisson's ratio effect of the structure through simulation. The results showed that the Poisson's ratio of the function primitive configuration designed with maximum flexibility was closer to zero, but the zero Poisson's ratio effect of a combination structure with positive and negative Poisson's ratios was unidirectional.

In the field of topology optimization, one of the commonly used microstructure design methods is the SIMP method [20], based on which previous researchers have investigated microstructures with limiting elastic properties [21], negative Poisson's ratio microstructures [22], microstructures with maximized bulk modulus and maximized shear modulus [23], and so on. While using the SIMP method to directly design zero Poisson's ratio structures, the whole optimization process will be unstable, and additional constraints must be added or the algorithm must be improved. Huang et al. [24] used the SIMP method to take the original zero Poisson's ratio configuration as a prototype, divided the whole structure into two parts, the design domain and the non-design domain, and designed a new zero Poisson's ratio configuration with the goal of volume minimization and the stiffness constraints as the condition, which improved the out-of-plane bending flexibility of the overall structure without reducing the transverse shear rigidity and bending stiffness, and the shortcoming of this method is that it is necessary to specify the initial configuration of the structure. Wang et al. [25] used the SIMP method and added weight factors to establish a multi stiffness topology model, and obtained a new zero Poisson's ratio honeycomb structure. It not only meets the in-plane stiffness requirements for deformation, but also gives the structure a specific load-bearing capacity, that is, high out of plane bending stiffness. Due to the need to consider the sensitivity of horizontal changes and vertical load-bearing capacity, a unidirectional zero Poisson's ratio microstructure was designed. Based on the homogenization method and SIMP method, Chen et al. [26] designed topological box structures with positive and negative Poisson's ratio effects, and then combined the positive and negative Poisson's ratio box structures to design a zero Poisson's ratio microstructure. The advantage of this is that it avoids the oscillation or convergence problems caused by directly optimizing the Poisson's ratio to zero, and can better perform comparative research and mechanism analysis. The disadvantage is that the zero Poisson's ratio structure cannot be designed directly, and due to this special design method, the zero Poisson's ratio effect of the designed zero Poisson's ratio structure is also unidirectional.

In summary, research combining topology optimization with zero Poisson's ratio microstructure design is limited. Direct design of zero Poisson's ratio structures requires further constraints or improved algorithms, including previous studies using multi-valued point function primitive topology optimization methods to design zero Poisson's ratio structures composed of positive and negative Poisson's ratio cell walls; Alternatively, the SIMP method can be used to design zero Poisson's ratio structures with new mechanical properties on the original zero Poisson's ratio configuration; And using weight factors

to establish a multi-stiffness topology model for designing zero Poisson's ratio honeycomb structures; Alternatively, it is possible to design positive and negative Poisson's ratio box structures, and then design a zero Poisson's ratio microstructure by combining the positive and negative Poisson's ratio box structures. However, there are still some limitations, such as high dependence on the initial design and unidirectional deformation of the structure.

In this paper, a zero Poisson's ratio topology optimization objective function was constructed based on the energy homogenization method. By using the boundary density evolution topology optimization method, microstructures with zero Poisson's ratio properties under different initial topologies and different volume fraction conditions are obtained. Finite element analysis was used to verify that the method proposed in this paper can effectively design microstructures with bidirectional zero Poisson's ratio properties.

The section arrangement of this article is as follows: In Section 2, a theoretical model for topology optimization of zero Poisson's ratio microstructures is proposed based on the energy homogenization method and boundary density evolution method. Section 3 presents numerical examples of topology optimization of zero Poisson's ratio microstructures under different initial design domains and different volume fractions. In Section 4, finite element simulation analysis is conducted on the examples, indicating that the method proposed in this paper can effectively design microstructures with expected stiffness and zero Poisson's ratio properties.

2 Topology optimization model for zero Poisson's ratio microstructures

2.1 Material interpolation model

In the topology optimization method based on element density, the element density is generally used as the design variable. At this time, the density corresponding to the material element is x_e , and Young's modulus of the element is usually defined by interpolation. In this paper, the same material interpolation model as the SIMP method [20] is used, and the elastic modulus of the element is expressed as:

$$E_e(x_e) = E_{\min} + x_e^p(E_0 - E_{\min}), \quad (1)$$

where E_0 is Young's modulus of the material, E_{\min} is a very small Young's modulus assigned to the void region to prevent singularity of the element stiffness matrix, and p is the penalty factor used to improve the stability of the algorithm.

2.2 Periodic boundary conditions

Due to the periodic arrangement of microstructures, it is necessary to ensure the stress and displacement continuity of the microstructure unit cell boundary. Under the assumption of periodicity and given strain ε_{ij}^0 , the displacement field of the basic unit can be written as the sum of the macroscopic displacement field and the

periodic fluctuation field u_i^* :

$$u_i = \varepsilon_{ij}^0 y_j + u_i^*. \quad (2)$$

However, in practical situations, since u_i^* is unknown, the equation cannot be directly imposed on the boundary. This general expression needs to be transformed into explicit boundary conditions. Xia et al. [23] proposed a unified periodic boundary condition for microstructure unit cells with paired and parallel boundaries based on the small deformation assumption as follows:

$$\begin{cases} u_i^{k+} = \varepsilon_{ij}^0 y_j^{k+} + u_i^* \\ u_i^{k-} = \varepsilon_{ij}^0 y_j^{k-} + u_i^* \end{cases}, \quad (3)$$

in the above equation, $k+$ and $k-$ represent the positive and negative directions along the y_j direction, respectively. Since the boundaries of the periodic microstructure unit cell are parallel, the u_i^* of the two can be eliminated by subtracting them as follows:

$$u_i^{k+} - u_i^{k-} = \varepsilon_{ij}^0 (y_j^{k+} - y_j^{k-}) = \varepsilon_{ij}^0 \Delta y_j^k = \omega_i^k, \quad (4)$$

for a periodic microstructure cell, Δy_j^k is a constant in equation (4). Given ε_{ij}^0 , the value on the right-hand side of the equation is a constant.

2.3 Material equivalent elasticity matrix

The homogenization method can establish the connection between the macro and micro scales and is the basis for the optimal design of microstructures. The basic idea of the homogenization method is given in Figure 2. It is assumed that the macrostructure is composed of composite materials whose equivalent properties can be calculated by the homogenization method [23].

In Figure 2, Γ represents the composite elastomer, f represents the body force, Γ_t represents the surface force applied, Γ_u denotes a given displacement boundary condition, x is a macroscopic variable, y is a local microscopic variable, and the local structure at a macroscopic point x can be viewed as consisting of a periodic arrangement of single cells.

According to the theory of asymptotic homogenization, the effective elastic tensor E_{ijkl}^H of periodic materials can be obtained as follows:

$$E_{ijkl}^H = \frac{1}{|Y|} \int_Y \left(\varepsilon_{pq}^{0(ij)} - \varepsilon_{pq}^{*(ij)} \right) E_{pqrs} \left(\varepsilon_{rs}^{0(kl)} - \varepsilon_{rs}^{*(kl)} \right) dY, \quad (5)$$

where $|Y|$ represents the area of the design domain of the periodic microstructure cell, $\varepsilon_{pq}^{0(ij)}$ is the element test strain field under periodic boundary conditions, with two independent vectors. $\varepsilon_{pq}^{*(ij)}$ is the unknown periodic fluctuation strain field generated by applying the element test strain, which can be obtained by solving the following

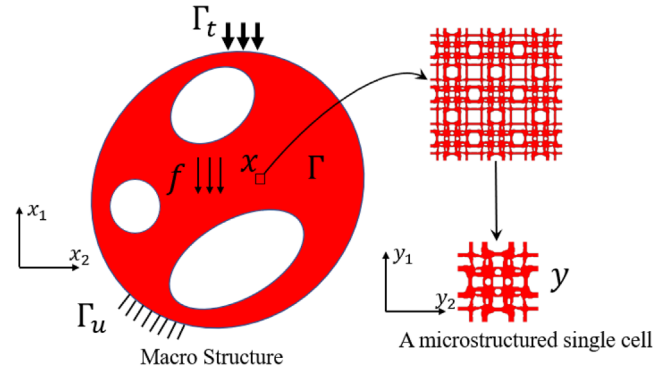


Fig. 2. Diagram of the idea of the homogenization method.

homogenization equation:

$$\int_Y \varepsilon_{pq}^{*(ij)} E_{pqrs} \frac{\partial v_i}{\partial y_j} dY = \int_Y \varepsilon_{pq}^{0(ij)} E_{pqrs} \frac{\partial v_i}{\partial y_j} dY. \quad (6)$$

The energy homogenization method [24] uses the principle of average stress and strain. By directly applying the unit test strain to the boundary of the basic unit, $\varepsilon_{pq}^{A(ij)}$ corresponding to the superimposed strain field $\left(\varepsilon_{pq}^{0(ij)} - \varepsilon_{pq}^{*(ij)} \right)$ in equation (5) can be derived, and the equivalent elastic tensor of the material microstructure can be rewritten as:

$$E_{ijkl}^H = \frac{1}{|Y|} \int_Y \varepsilon_{pq}^{A(ij)} E_{pqrs} \varepsilon_{rs}^{A(kl)} dY. \quad (7)$$

In finite element analysis, the basic unit is discretized into N elements, and equation (7) can be approximately represented as:

$$E_{ijkl}^H = \frac{1}{|Y|} \sum_{e=1}^N \left(u_e^{A(ij)} \right)^T k_e u_e^{A(kl)}, \quad (8)$$

where $u_e^{A(kl)}$ is the unit displacement solution for the corresponding unit test strain $\varepsilon^{0(kl)}$, k_e is the element stiffness matrix. In the case of two-dimensional structures, it can be noted that the subscript correspondence relationship is 11→1, 22→2, 12→3, and equation (8) can be expanded as:

$$E^H = \begin{bmatrix} E_{11}^H & E_{12}^H & E_{13}^H \\ E_{21}^H & E_{22}^H & E_{23}^H \\ E_{31}^H & E_{32}^H & E_{33}^H \end{bmatrix} = \begin{bmatrix} Q_{11} & Q_{12} & Q_{13} \\ Q_{21} & Q_{22} & Q_{23} \\ Q_{31} & Q_{32} & Q_{33} \end{bmatrix}, \quad (9)$$

where Q_{ij} is the strain energy of a single cell and can be expressed as:

$$Q_{ij} = \frac{1}{|Y|} \sum_{e=1}^N q_e^{(ij)}, \quad (10)$$

are the sums of element mutual energies $q_e^{(ij)}$:

$$q_e^{(ij)} = \left(u_e^{A(i)} \right)^T k_e u_e^{A(j)}. \quad (11)$$

2.4 Zero Poisson's ratio microstructure topology optimization model

This article presents a topology optimization design for materials with zero Poisson's ratio. According to the definition of Poisson's ratio, it can be calculated as follows:

$$\mu_{12}^H = \frac{E_{1122}^H}{E_{1111}^H}, \mu_{21}^H = \frac{E_{2211}^H}{E_{2222}^H}. \quad (12)$$

If the above formula is directly used as the objective function, the entire optimization process may not be stable. Therefore, this paper proposes an equivalent expression for zero Poisson's ratio as follows:

$$c = E_{1122}^H{}^2 + E_{2211}^H{}^2 - 0.9^{G_f} (E_{1111}^H + E_{2222}^H), \quad (13)$$

where c is the objective function for optimization, and G_f is the iteration step.

During the entire optimization process, as the number of iterations increases, the values of E_{1122}^H and E_{2211}^H become smaller and smaller, while the values of E_{1111}^H and E_{2222}^H become larger and larger, which makes the Poisson's ratio of the microstructure closer to zero. Therefore, the mathematical model for topology optimization of zero Poisson's ratio microstructures can be expressed as:

$$\begin{cases} \min c = E_{1122}^H{}^2 + E_{2211}^H{}^2 - 0.9^{G_f} (E_{1111}^H + E_{2222}^H) \\ \text{s.t. } V(x_e) \leq V_0 \\ 0 < x_{\min} \leq x_e \leq 1 \end{cases} \quad (14)$$

where c is the optimization objective function, E_{ijkl}^H is the microstructure's equivalent elastic tensor, $V(x_e)$ is the volume of the microstructure, V_0 is the volume constraint, and x_e is the density of the element.

2.5 Sensitivity filtering and density filtering for boundary density evolution optimization method

To ensure the existence of a reasonable solution and avoid checkerboard patterns in topology optimization problems, some constraints must be applied to the optimization process. A common method is sensitivity filtering [27], which can be expressed as follows:

$$\frac{\partial c}{\partial x_e} = \frac{1}{\max(\gamma, x_e) \sum_{i \in N_e} H_{ei}} \sum_{i \in N_e} H_{ei} x_i \frac{\partial c}{\partial x_e}, \quad (15)$$

where N_e denotes the set of all elements within a straight line distance from the center of elements e within the filtering radius; γ is a lower bound given to avoid 0 in the denominator; and H_{ei} is a weight factor denoting the weight

that each element i occupies within the filtering radius, defined as:

$$H_{ei} = \max(0, r_{\min} - \Delta(e, i)), \quad (16)$$

where $\Delta(e, i)$ represents the distance between the center points of element e and element i .

To improve the instability of the SIMP method in optimizing zero Poisson's ratio structures and to enhance computational efficiency, this paper adopts the boundary density evolution optimization method with boundary density hierarchical filtering [28], which can perfectly solve the problem of gray elements and converge quickly. The specific algorithm is as follows:

$$\begin{aligned} a_0 &= \left[0 : \frac{1}{G_f} : 1 \right] \\ a_1 &= \text{find}(x_e^{\text{new}} \leq a_0(\text{loop})) \\ x_e^{\text{new}}(a_1) &= 0, \end{aligned} \quad (17)$$

where a_0 is an intermediate parameter, G_f is the density filter grading factor, x_e^{new} is the updated design variable, loop is the number of loops, and a_1 is the element number corresponding to the design variable less than $a_0(\text{loop})$ in the current loop step.

2.6 Optimal criterion algorithms

For optimization problems, such as the one presented in equation (17), the optimal criterion algorithm is typically chosen due to its stability and efficiency. The design variables are updated using the strategy outlined in reference [27]:

$$x_e^{\text{new}} = \begin{cases} \max(0, x_e - m) & \text{if } x_e B_e^\eta \leq \max(0, x_e - m) \\ \min(1, x_e + m) & \text{if } x_e B_e^\eta \geq \min(1, x_e - m) \\ x_e B_e^\eta & \text{otherwise} \end{cases} \quad (18)$$

where m is the movement limit value, η is the numerical damping factor and B_e is determined by the optimal conditions as follows:

$$B_e = -\frac{\partial c}{\partial x_e} / \lambda \frac{\partial V}{\partial x_e}, \quad (19)$$

where the Lagrange multiplier λ must satisfy the volume constraint condition, and its specific value can be determined using the dichotomy algorithm.

The sensitivity of the objective function $\partial c / \partial x_e$ can be calculated using the adjoint method [27]:

$$\frac{\partial E_{ijkl}^H}{\partial x_e} = \frac{1}{|Y|} p x_e^{p-1} (E_0 - E_{\min}) \left(u_e^{A(ij)} \right)^T k_0 u_e^{A(ij)}, \quad (20)$$

where k_0 is the element stiffness matrix of elements with unit Young's modulus. The structure is uniformly meshed into finite elements and the volume v_e of each element is set

to 1, therefore the sensitivity of the volume constraint to the design variable is:

$$\frac{\partial v}{\partial x_e} = 1. \quad (21)$$

2.7 Boundary smoothing

If finite element results are output directly, the boundary of the microstructure will appear jagged, which is not convenient for the subsequent 3D printing of metamaterials. It is necessary to smooth the boundary of the microstructure. This article mainly uses element density to convert to node density and then uses the node density level set to display the boundary of the microstructure. Node density can be obtained by interpolation from element density. Taking the structure of the four elements shown in Figure 3 as an example of a two-dimensional plane problem, the formula for converting element density to node element density is as follows:

$$D_1 = x_1, D_2 = (x_1 + x_2)/2, D_3 = x_2, D_4 = (x_1 + x_3)/2, D_5 = (x_1 + x_2 + x_3 + x_4)/4,$$

$$D_6 = (x_2 + x_4)/2, D_7 = x_3, D_8 = (x_3 + x_4)/2, D_9 = x_4, \quad (22)$$

where $x_i (i=1,2,3,4)$ represents the density of each element, and $D_i (i=1,2,3,\dots,9)$ represents the density of each node.

The boundary of the microstructure can be defined by utilizing a node density level set as follows:

$$\begin{cases} D_i > S, i \in \Omega \\ D_i = S, i \in \Gamma \\ D_i < S, i \in D \setminus \Omega \end{cases}, \quad (23)$$

in which D_i represents node density, Ω represents the solid design domain, Γ represents the boundary design domain, $D \setminus \Omega$ represents the hollow design domain, and S represents the level set value.

After using the node density level set to perform smoothing on the microstructure, there may be some errors between Poisson's ratio of the microstructure models and the original results. Therefore, it is necessary to fine-tune the level set values of the node density to obtain a microstructure model with a Poisson's ratio closer to zero. The details are shown in the example later.

3 Numerical example of zero Poisson's ratio microstructure design

This section focuses on the topology optimization design of microstructures with zero Poisson's ratio. Specific examples are given for different initial topologies and volume fractions, and the influence of different initial topologies and volume fractions on the designed microstructures with zero Poisson's ratio is discussed.

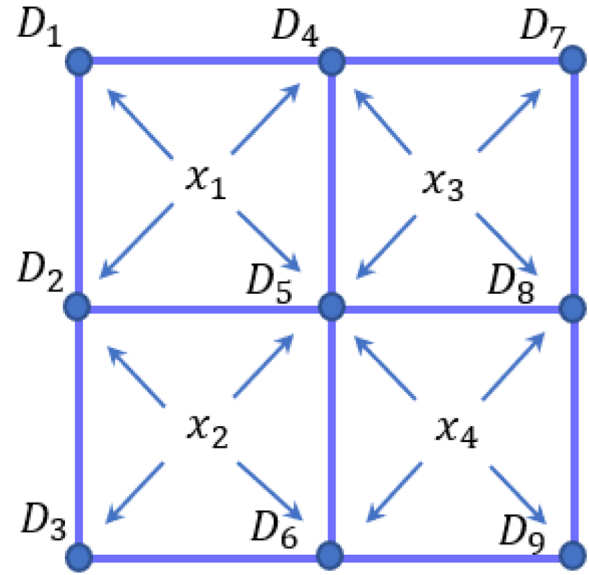


Fig. 3. Example diagram of a four-node element in two-dimensional plane.

3.1 Zero Poisson's ratio microstructure designs in different initial design domains

Assuming a material volume fraction of 0.5 and Young's modulus of 1 and Poisson's ratio of 0.3 for the solid material, and using a finite element mesh of 100×100 , the microstructure is topologically optimized. Table 1 shows the optimization results for three different initial design domains.



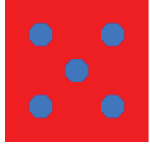

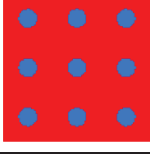
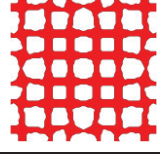
It is easy to see from Table 1 that the initial design domain of the material has a certain influence on the topological structure of the final optimized structure. In the actual optimization process, there are many different local optimal solutions due to topological optimization, and there are also many possible results for the topological optimization of the microstructure. However, the resulting Poisson's ratio is close to zero in all cases.

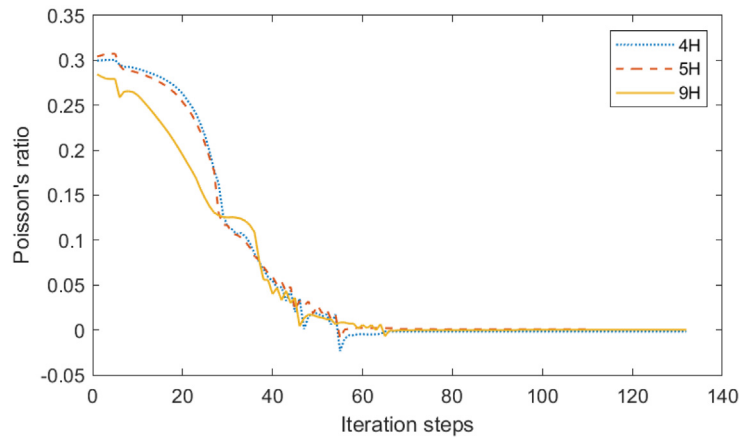
Figure 4 shows the iteration optimization curves of Poisson's ratio for microstructures with different initial design domains. It can be seen from the figure that Poisson's ratio iteration curves of the microstructures corresponding to different initial design domains are different during the optimization process. However, as the number of iterations increases, the Poisson's ratio finally converges to a value close to zero, and a microstructure with zero Poisson's ratio characteristics is generated. It can be seen that when the iteration step reaches about 60 steps, the Poisson's ratio begins to remain around 0, reflecting the stability of the algorithm.

3.2 Zero Poisson's ratio microstructure designs with different volume fractions

To further discuss the influence of volume fraction on the topological optimization results, the volume fractions are set to 0.4, 0.5, and 0.6, respectively. The optimization results are shown in Table 2.

Table 1. The optimization results for three different initial design domains.

Initial design domains	Optimization results	Equivalent elastic tensor	Poisson's ratio
		$\begin{bmatrix} 0.2379 & -0.0004 & 0.0000 \\ -0.0004 & 0.2379 & 0.0000 \\ 0.0000 & -0.0000 & 0.0171 \end{bmatrix}$	0.002
		$\begin{bmatrix} 0.2421 & 0.0002 & -0.0000 \\ 0.0002 & 0.2421 & -0.0000 \\ -0.0000 & -0.0000 & 0.0124 \end{bmatrix}$	0.001
		$\begin{bmatrix} 0.2507 & 0.0001 & -0.0000 \\ 0.0001 & 0.2507 & -0.0000 \\ -0.0000 & -0.0000 & 0.0204 \end{bmatrix}$	0.0004

**Fig. 4.** Iteration optimization curves of Poisson's ratio for microstructures with different initial design domains.

It can be seen from Table 2 that the optimization results for different volume fractions are similar to those for different initial design domains, that is, the topological structures of the microstructures are different for different volume fractions, but their Poisson's ratio values are all close to 0.

Figure 5 presents the iteration optimization curves of Poisson's ratio for microstructures with different volume fractions. As can be observed from Figure 5, similar to Figure 4, the Poisson's ratio of the microstructure also stabilizes around 0 when the iteration steps reach around 60, further indicating the stability of the algorithm.

4 Experiment simulation and analysis

To validate the zero Poisson's ratio characteristic of the microstructure, the designed microstructure model is imported into ABAQUS for analysis. The element chosen is quadrilateral, and the elastic modulus and initial


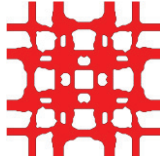

Poisson's ratio are consistent with the conditions during optimization. The boundary conditions are set by fixing the horizontal displacement of the middle vertical nodes, as well as the vertical displacement of the middle horizontal node. Then, the top and bottom boundaries are loaded, and the equivalent Poisson's ratio is calculated as the ratio of the average displacement of the left and upper adjacent edges.

Figure 6 shows the microstructure simulation model.

4.1 Analysis of mechanical properties of zero Poisson's ratio microstructures with different initial design domains

After using node density level sets to smooth the boundaries of microstructures, there will be some errors between the Poisson's ratio of the microstructure model and the original results. Therefore, this error can be reduced by adjusting the level set values.

Table 2. Optimization results of zero Poisson's ratio microstructures with three different volume fractions.

Volume fractions	Optimization results	Equivalent elastic tensor	Poisson's ratio
0.4		$\begin{bmatrix} 0.1949 & -0.0002 & 0.0000 \\ -0.0002 & 0.1949 & 0.0000 \\ 0.0000 & 0.0000 & 0.0041 \end{bmatrix}$	-0.001
0.5		$\begin{bmatrix} 0.2421 & 0.0002 & -0.0000 \\ 0.0002 & 0.2421 & -0.0000 \\ -0.0000 & -0.0000 & 0.0124 \end{bmatrix}$	0.001
0.6		$\begin{bmatrix} 0.3190 & -0.0002 & 0.0000 \\ -0.0002 & 0.3190 & 0.0000 \\ -0.0000 & -0.0000 & 0.0284 \end{bmatrix}$	-0.001

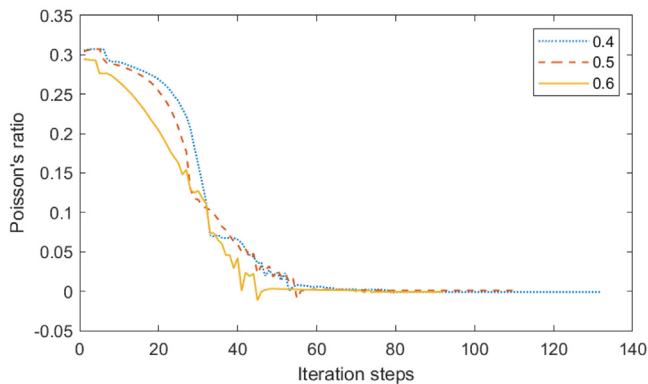
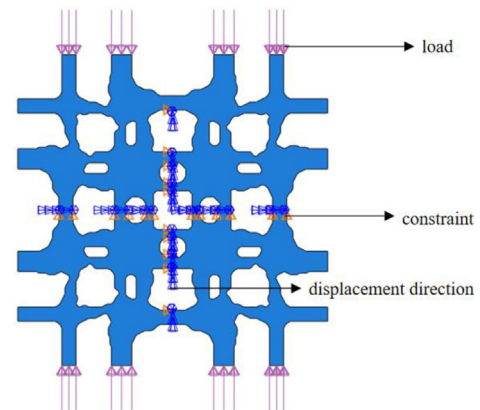
**Fig. 5.** Iteration optimization curves of Poisson's ratio for microstructures with different volume fractions.

Table 3 shows the deformation cloud maps and corresponding equivalent Poisson's ratios (EPR) of microstructure simulation models with different initial design domains before and after modification of the level set values. As shown in Table 3, the number outside the parentheses below each deformation cloud map represents its level set value, and the number inside the parentheses represents the volume fraction of the microstructure.

The conclusions that can be drawn from Table 3 are as follows:


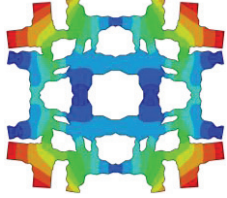
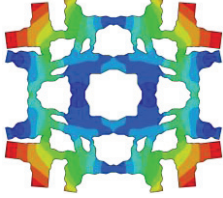

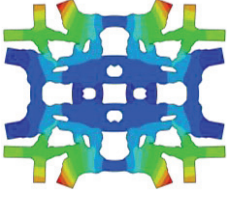
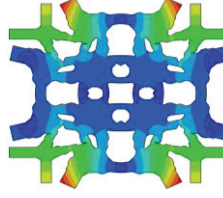

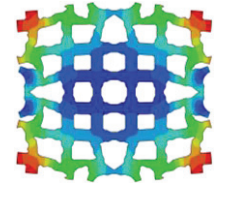
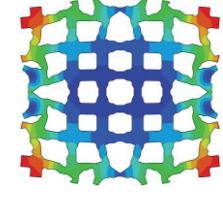
- If the level set values are not fine-tuned, the microstructure's equivalent Poisson's ratio is also close to 0, but with a slightly larger error.
- The equivalent Poisson's ratio of the model and the optimized finite element results have a certain error due to the smooth treatment of the model boundary. Fine-tuning the level set values can reduce this error. Table 3 shows that, upon adjusting the level set value, the volume fraction of the optimized structure with

**Fig. 6.** The microstructure simulation model.

initial topology of four, five, and nine holes accounts for 94.2%, 94.3%, and 92.9% of the original volume, respectively. However, the Poisson's ratio of the structure is only 25%, 6.3%, and 9.5% of that of the original structure, respectively. By adjusting the level set value of the original structure, the error due to the boundary smoothing treatment can be reduced, resulting in a Poisson's ratio that is closer to the optimization result.

- The deformation patterns of the microstructures with three different initial topologies, as shown in the deformation cloud maps, all meet the deformation mode of zero Poisson's ratio materials. This means that when compressed or stretched in one direction, there is neither stretching nor contraction in the other direction. Different initial topologies have almost no effect on the equivalent Poisson's ratio of the material, as seen from their equivalent Poisson's ratios. This

Table 3. Deformation cloud maps of microstructures with different initial design domains.

Initial design domain	Before modification		After modification	
	Deformation cloud map	EPR	Deformation cloud map	EPR
	 0.5(0.504)	0.024	 0.62(0.475)	0.006
	 0.5(0.506)	0.032	 0.61(0.477)	0.002
	 0.5(0.508)	0.042	 0.61(0.472)	0.004

indicates that the method proposed in this paper is effective in designing microstructures with zero Poisson's ratio characteristics.

4.2 Analysis of mechanical properties of zero Poisson's ratio microstructures with different volume fractions

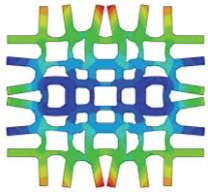
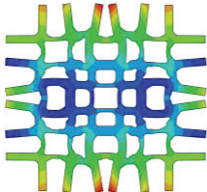
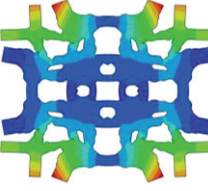
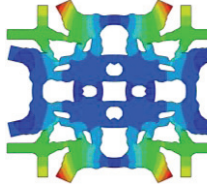
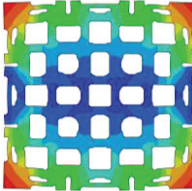
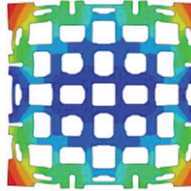
The preceding section discussed how different initial design domains affect the microstructural characteristics of zero Poisson's ratio in a design. This section focuses on the effects of varying volume fractions on the mechanical properties of microstructures with zero Poisson's ratio. Table 4 displays the deformation cloud maps and equivalent Poisson's ratios of microstructures with different volume fractions, before and after modifying the level set values. The number outside the parentheses below each deformation cloud map represents its level set value, while the number inside the parentheses represents the volume fraction of the microstructure. From Table 4, it is evident that the mechanical properties of microstructures under different volume fractions still conform to the zero Poisson's ratio requirement. Similar to the case of different

initial design domains, varying volume fractions have little impact on the zero Poisson's ratio of the microstructure, which remains close to zero. Moreover, fine-tuning the level set values can reduce errors caused by boundary smoothing processing.

The conclusions that can be drawn from Table 4 are as follows:

- Table 4 shows that the mechanical properties of microstructures with different volume fractions still satisfy zero Poisson's ratio performance. Similar to the case of different initial design domains, the different volume fractions have almost no effect on the zero Poisson's ratio performance of the microstructures, which remains close to zero. By adjusting the level set values, the structures with volume fractions of 0.4, 0.5, and 0.6 were fine-tuned to 93.6%, 94.3%, and 91.3% of the original volume fractions, respectively. The Poisson's ratios were also adjusted to 4.2%, 6.3%, and 38.1% of the original values. Similar to the results in Table 3, demonstrating that adjusting the level set values effectively reduces the error caused by boundary smoothing treatment. This leads to a Poisson's ratio that is closer to the optimized value.

Table 4. Deformation cloud maps of microstructures with different volume fractions.

Volume fractions	Before modification		After modification	
	Deformation cloud map	EPR	Deformation cloud map	EPR
0.4	 0.5(0.407)	0.024	 0.57(0.381)	0.001
0.5	 0.5(0.506)	0.032	 0.61(0.477)	0.002
0.6	 0.5(0.609)	0.042	 0.65(0.556)	0.016

– From the viewpoint of the deformation mechanism, most of the traditional zero Poisson ratio honeycomb structures are only unidirectional zero Poisson’s ratio effect, and their deformation mechanism is to form the zero Poisson’s ratio effect through the deformation rotation of the rods inside the structure. The microstructured metamaterials with bi-directional zero Poisson’s ratio effect obtained by the optimization of the method in this paper are mainly formed by some horizontal and vertical rods through the nodes of specific shapes, and the characteristics of the structural composition are similar to the structure designed by Anders Clausen et al. [18]. All of them are formed by the crossing of horizontal and vertical rods after bending and deformation.

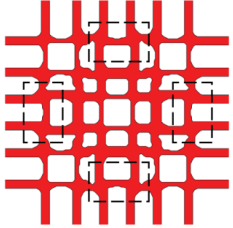
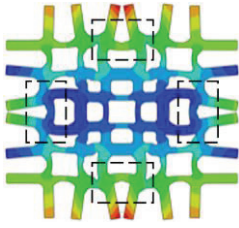
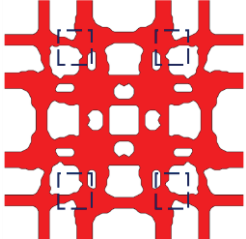
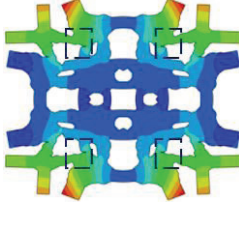
Table 5 presents a comparison chart of microstructure deformation before and after.

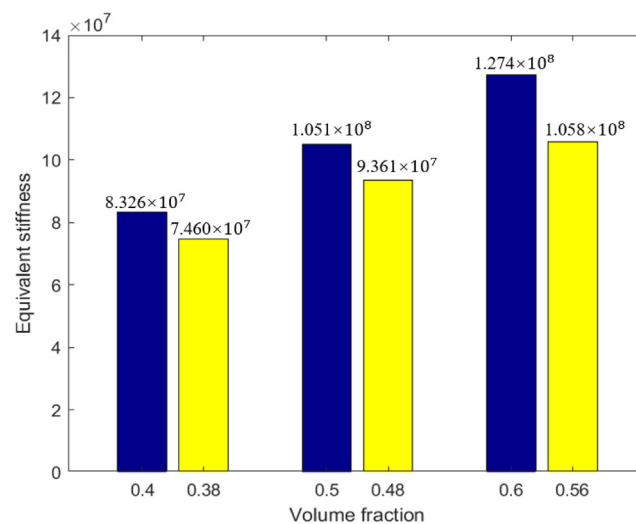
As can be seen from Table 5, when the pressure is applied to the vertical direction, some locally curved places of the original structural rods will be changed from the original curve to the shape close to a straight line because of the force, and some nodes will produce a certain degree of

rotation, and the combined effect of both cancels out the deformation of the structure originally to be outwardly extended, so in the deformation of the force, it is mainly the rods and the nodes that bear most of the deformation, so that the structure has a zero Poisson’s ratio effect and the color of the deformation cloud graph shows that the vertical rod bears most of the loads throughout the stressing process, so this paper’s microstructures have a large stiffness at the same time as they have a zero Poisson’s ratio effect.

To investigate the effect of volume fraction on the stiffness of the microstructure, further analysis was carried out on the stress and deformation of the microstructure. The change in stiffness was measured using equivalent stiffness, which is equal to the ratio of vertical load to vertical displacement. Figure 7 shows the equivalent stiffness of microstructures with different volume fractions before and after adjusting the level set values. The blue part represents the equivalent stiffness of the microstructure before the level set values are modified, and the yellow part represents the equivalent stiffness after modification.

Table 5. Comparison of microstructure before and after deformation.

Deformation mode	Undeformed microstructure	Microstructure after deformation
Node Rotation		
Localized deformation of rods		





 Microstructure before modification  Microstructure after modification

Fig. 7. Equivalent stiffness maps of microstructures in Table 4 with different volume fractions before and after modification of the level set values.

As can be seen in Figure 7, the stiffness of the microstructure decreases with decreasing volume fraction. However, after the modification of the level set value, the stiffness of the structure changes but its zero Poisson's ratio property remains stable. Therefore, by choosing the appropriate volume fraction of the material and adjusting the level set value, zero Poisson's ratio metamaterials with desired stiffness can be designed.

4.3 Mechanical performance analysis of zero Poisson's ratio metamaterials

To demonstrate that the multicellular structure obtained through the method proposed in this paper also has zero

Poisson's ratio characteristics, single cells are arranged and combined to form multicellular metamaterials. Then, finite element analysis is used to analyze it in both the X and Y directions. Due to the symmetric constraints on the structure, the structural constraints remain unchanged, and the load changes from vertical to horizontal. Tables 6 and 7 show the microstructural deformation cloud maps and equivalent Poisson's ratios of single-cell and multicellular structures with volume fractions of 0.4 and 0.5 under compression in the Y and X directions, respectively.

According to Table 6, it is evident that the equivalent Poisson's ratio of the structure increases to some extent as the single cell is converted to a multi-cell structure. The increase in Poisson's ratio is due to the change in the

Table 6. Deformation maps and Poisson’s ratios of single-cell and multi-lattice structures with zero Poisson’s ratio at different volume fractions in the X direction.

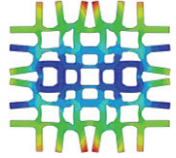
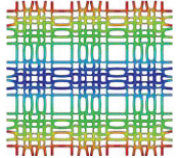
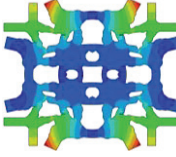
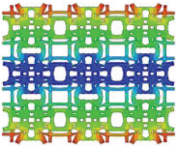
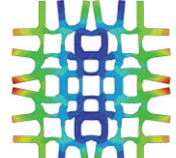
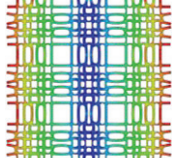
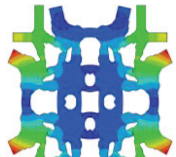
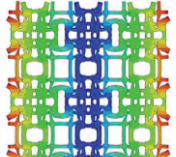
Volume fraction	1×1		3×3	
	Deformation cloud map	EPR	Deformation cloud map	EPR
0.4		0.001		0.01
0.5		0.002		0.01

Table 7. Deformation maps and Poisson’s ratios of single cell and multi-lattice structures with zero Poisson’s ratio for different volume fractions in the Y direction.

Volume fraction	1×1		3×3	
	Deformation cloud map	EPR	Deformation cloud map	EPR
0.4		-0.002		0.008
0.5		0.004		0.01

structure size and the number of finite element cells when converting from a unicellular structure to a multicellular structure, which leads to a certain amount of error. Nevertheless, the overall Poisson’s ratio of the structure remains close to zero.

Table 7 shows that periodic microstructures with zero Poisson’s ratio can be combined to form metamaterials with zero Poisson’s ratio properties in both directions. The slightly different results in both directions are because the whole model has a slight error in the optimization process and is not ideally perfectly symmetric.

5 Conclusion

This paper proposes a topology optimization objective function for zero Poisson’s ratio, and obtains microstructures with zero Poisson’s ratio performance under different initial topologies and volume fraction conditions through the boundary density evolution topology optimization method. Due to the existence of errors between the microstructure model after boundary smoothing and the initial optimization result, a more reasonable microstructure model can be obtained by fine-tuning

the node density level set value to reduce this error. Mechanical performance analyses of microstructure models under different conditions show that the initial design domain and volume fraction have almost no effect on the zero Poisson's ratio performance of the microstructure. The proposed method can effectively design microstructures with stable zero Poisson's ratio performance. Meanwhile, the examples also show that by selecting appropriate volume fractions and materials, microstructures with expected stiffness and zero Poisson's ratio performance can be designed. When the microstructure unit cell is combined into a multi-cell metamaterial through periodic arrangement, the overall Poisson's ratio of the entire structure still tends to zero, indicating that the proposed method can effectively design 2D metamaterials with bi-directional zero Poisson's ratio performance. Subsequently, the topology optimization design of 3D zero Poisson's ratio metamaterials will be further studied.

Funding

This research was supported by the National Natural Science Foundation of China (12072114), Guangdong Basic and Applied Basic Research Foundation (2023A1515012830), and the Guangdong Provincial Key Laboratory of Modern Civil Engineering Technology (2021B1212040003).

Conflicts of interest

The authors declare that they have no known competing financial interests or personal relationships that could have appeared to influence the work reported in this paper.

Data availability statement

All data in this article can be obtained under reasonable request.

Author contribution statement

Xueping Li: Conceptualization, Validation, Methodology, Supervision, Writing – review & editing. Jiajun Zhu: Data curation, Investigation, Methodology, Writing – original draft. Peng Wei: Conceptualization, Methodology, Supervision, Writing – review & editing. Cheng Su: Conceptualization, Methodology, Supervision.

References

- O. Sigmund, Materials with prescribed constitutive parameters: An inverse homogenization problem, *Int. J. Solids Struct.* **31**, 2313–2329 (1994)
- I.E. Khadiri, M. Zemzami, N.Q. Nguyen, M. Abouelmajd, N. Hmina, S. Belhouideg, Topology optimization methods for additive manufacturing: a review, *Int. J. Simul. Multidisci. Des. Optim.* **14**, 12 (2023)
- P. Wei, Y. Liu, Z.Y. Li, A multi-discretization scheme for topology optimization based on the parameterized level set method, *Int. J. Simul. Multidisci. Des. Optim.* **11**, 3 (2020)
- W. Jiang, H. Ma, J. Wang, J.F. Wang, M.D. Feng, S.B. Qu, Mechanical metamaterial with negative Poisson's ratio based on circular honeycomb core, *Chin. Sci. Bull.* **61**, 1421–1427 (2016)
- X. Li, R. Xiao, J.Z. Chen, J.Q. Li, R. Fan, J. Song, Y. Lu, Plate-based cylinder metamaterial with negative Poisson's ratio and outstanding mechanical performance, *Int. J. Simul. Multidisci. Des. Optim.* **66**, 793–806 (2023)
- W.Y. Zhang, Development and application of metamaterials, *Mag. Equip. Mach.* **16**, 67–71 (2018)
- K.R. Olympic, F. Gandhi, Zero Poisson's ratio cellular honeycombs for flex skins undergoing one-dimensional morphing, *J. Intell. Mater. Syst. Struct.* **21**, 1737–1753 (2010)
- J.N. Grima, L. Oliveri, D. Attard, B. Ellul, R. Gatt, G. Cicala, G. Recca, Hexagonal honeycombs with zero Poisson's ratios and enhanced stiffness, *Adv. Eng. Mater.* **12**, 855–862 (2010)
- C. Lu, Y.X. Li, E.B. Dong, J. Yang, Equivalent elastic modulus of zero Poisson's ratio honeycomb core, *J. Mater. Eng.* **3**, 80–84 (2013)
- J.F. Li, X. Shen, J. Chen, Single cells' in-plane equivalent moduli analysis of zero Poisson's ratio cellular structures and their effects factor, *Acta Aeronaut. Astronaut. Sin.* **36**, 3616–3629 (2015)
- D.B. Simone, L. Susanna, S. Fabrizio, AUXHEX-A Kirigami inspired zero Poisson's ratio cellular structure, *Compos. Struct.* **176**, 433–441 (2017)
- X.B. Gong, J. Huang, F. Scarpa, Y.J. Liu, J.S. Leng, Zero Poisson's ratio cellular structure for two-dimensional morphing applications, *Compos. Struct.* **134**, 384–392 (2015)
- W.J. Cheng, L. Zhou, P. Zhang, T. Qiu, Design and analysis of a zero Poisson's ratio mixed cruciform honeycomb and its application in flexible skin, *Acta Aeronaut. Astronaut. Sin.* **36**, 680–690 (2015)
- Y.F. Chang, H. Wang, Q.X. Dong, Machine learning-based inverse design of auxetic metamaterial with zero Poisson's ratio, *Mater. Today Commun.* **30**, 103186 (2022)
- R. Hamzehei, A. Serjouei, N. Wu, A. Zolfagharian, M. Bodaghi, 4D metamaterials with zero Poisson's ratio, shape recovery, and energy absorption features, *Adv. Eng. Mater.* **24**, 2270037 (2022)
- X. Chen, M.H. Fu, W.H. Li, V.S. Sheshenin, An unusual 3D metamaterial with zero Poisson's ratio in partial directions, *Adv. Eng. Mater.* **23**, 2001491 (2021)
- V. Gaal, V. Rodrigues, O.S. Dantas, S.D. Galvão, F.A. Fonseca, New zero Poisson's ratio structures, *Phys. Status Solidi RRL* **14**, 1900564 (2020)
- A. Clausen, F.W. Wang, J.S. Jensen, O. Sigmund, J.A. Lewis, Topology optimized architectures with programmable Poisson's ratio over large deformations, *Adv. Mater.* **27**, 5523–5527 (2015)
- D.Q. Yang, S. Zhong, Functional element topology optimization method based on multiple evaluation points for metamaterial design with zero Poisson's ratio, *Acta Mater. Compositae Sin.* **37**, 3229–3241 (2020)
- M.P. Bendsøe, O. Sigmund, Material interpolation schemes in topology optimization. *Arch Appl Mech.* **69**, 635–654 (1999).

21. Y. Zhang, Y.X. Du, D.X. Du, Q.H. Tian, Topology optimization for material microstructures with extreme elastic properties, *J. China Three Gorges Univ., Nat. Sci.* **38**, 71–74 (2016)
22. Y.X. Du, R. Li, M. Xu, Q.H. Tian, X.M. Zhou, Topology optimization design for negative Poisson's ratio microstructure, *J. Eng. Des.* **25**, 450–456 (2018)
23. L. Xia, P. Breitkopf, Design of materials using topology optimization and energy-based homogenization approach in Matlab, *Struct. Multidiscipl Optim.* **52**, 1229–1241 (2015)
24. J. Huang, Q.H. Zhang, F. Scarpa, Y.J. Liu, J.S. Leng, Multi-stiffness topology optimization of zero Poisson's ratio cellular structures, *Composites Part B* **140**, 35–43 (2018)
25. W. Wang, Design and application of zero Poisson's ratio honeycomb structure, Dalian University of Technology (2019)
26. Y. Chen, L. Ye, X. Han, Experimental and numerical investigation of zero Poisson's ratio structures achieved by topological design and 3D printing of SCF/PA, *Compos. Struct.* **293**, 115717 (2022)
27. M.P. Bendsøe, O. Sigmund, *Topology Optimization: Theory, Method and Applications*. Springer (2003)
28. X.P. Li, C.H. Qin, P. Wei, C. Su, A boundary density evolutionary topology optimization of continuum structures with smooth boundaries, *Int. J. Numer. Meth. Eng.* **123**, 158–179 (2022)

Cite this article as: Xueping Li, Jiajun Zhu, Peng Wei, Cheng Su, Topology optimization design of microstructures with zero Poisson's ratio, *Int. J. Simul. Multidisci. Des. Optim.* **15**, 12 (2024)